CrossMark

Dominant negative Poynting effect in simple shearing of soft tissues

M. Destrade · C. O. Horgan · J. G. Murphy

Abstract   We identify three distinct shearing modes for simple shear deformations of transversely isotropic soft tissue which allow for both positive and negative Poynting effects (that is, they require compressive and tensile lateral normal stresses, respectively, in order to maintain simple shear). The positive Poynting effect is that usually found for isotropic rubber. Here, specialisation of the general results to three strain-energy functions which are quadratic in the anisotropic invariants, linear in the isotropic strain invariants and consistent with the linear theory suggests that there are two Poynting effects which can accompany the shearing of soft tissue: a dominant negative effect in one mode of shear and a relatively small positive effect in the other two modes. We propose that the relative inextensibility of the fibres relative to the matrix is the primary mechanism behind this large negative Poynting effect.

Keywords   Elasticity · Modelling · Poynting effect · Simple shear · Soft tissue · Transverse isotropy

1 Introduction

Shearing deformations of soft tissue have been somewhat neglected in the literature, from both experimental and modelling points of view, and are far less common than the almost ubiquitous tensile and biaxial material characterisation tests. However, the large shear of a soft material is a most illuminating testing protocol. Simple shear is achieved by gluing two opposite sides of a cuboid sample to two flat rigid platens and by displacing one platen parallel to the other [1]. What becomes quickly apparent, both in practice and in theory, is that this displacement is achieved by applying a force in the direction of shear (the direction of motion of the moving platen) and forces in the direction normal to the platens. For isotropic materials, Poynting [2] showed experimentally, and Rivlin [3] theoretically, that the normal forces had to be compressive on the platens because simple shear causes

M. Destrade · J. G. Murphy (✉)
School of Mathematics, Statistics and Applied Mathematics, National University of Ireland Galway, Galway, Ireland
e-mail: jeremiah.murphy@dcu.ie

C. O. Horgan
School of Engineering and Applied Science, University of Virginia, Charlottesville, VA 22904, USA

J. G. Murphy
Centre for Medical Engineering Research, Dublin City University, Glasnevin, Dublin 9, Ireland

the sample to expand in the direction normal to these platens. Although Poynting [2] demonstrated this normal stress effect for pure torsion, the tendency of a cuboid to expand in simple shear is now widely called the *positive Poynting effect*. Recent contributions on the topic include those by Mihai and Goriely [4], Destrade et al. [5] and Horgan and Smayda [6].

Although it is generally accepted that most existing isotropic materials exhibit the *positive* Poynting effect, the experimental data of Janmey et al. [7] suggest that biogels reinforced with biological macromolecules such as fibrin display a *negative* Poynting effect, i.e., there is a tendency for the platens to move closer together when subjected to large shears. Several different approaches could be adopted to model this unexpected behaviour. For example, one could relax some of the usual conditions imposed on the material response, such as the empirical inequalities, or, alternatively, allow for some degree of compressibility, field inhomogeneity, anisotropy, or swelling, for example. The work of Destrade et al. [8], Horgan and Murphy [9], Mihai and Goriely [4] and Wu and Kirchner [10], for instance, is illustrative of these different methods. One could also exploit the microstructure of the reinforced biogels, noting that they are composed of semi-flexible filaments embedded in a soft matrix. Although the filaments are distributed isotropically in every direction, they behave differently in traction (strong resistance) than in compression (high compliance), and the contribution of the stretched filaments can dominate the overall response. Thus, in simple shear, the strong pull of the fibres can overcome the weaker push of the compressed fibers in the sheared matrix and therefore bring the platens together. This avenue of microstructural modelling was explored by Janmey et al. [7] and Ogden (private communication). Here we propose that the same effect can be modelled using the phenomenological theory developed by Spencer [11] for strong fibres embedded in an isotropic matrix.

Hence we assume homogeneity, incompressibility and *transverse isotropy*, so that the mechanical response of the solid is influenced by a single preferred direction (Sect. 2). We use material models (introduced by Murphy [12]) which are compatible with linear anisotropic elasticity in the infinitesimal regime. Such consistency with the linear theory is supported by extensive experimental data, particularly for muscles. The models considered are likely to be good models of the mechanical response of soft tissue in general, given that they are guaranteed to model infinitesimal deformations accurately and that typical physiological strains are only of the order of 10 %.

The systematic, comprehensive testing regime for the shearing of soft tissue introduced by Dokos et al. [13] is considered in Sect. 3, with three distinct physical modes of shear identified, and we compute the corresponding stress components. We show that general considerations of the normal stresses that accompany shearing suggest the existence of both positive and negative Poynting effects, but with the negative effect dominant. This large negative Poynting effect occurs only for one of the three modes of shear: it occurs when fibres are originally normal to the platens. This is because the fibres strongly resist the stretch imposed upon them by the shearing deformation and overcome the response of the soft isotropic matrix, with the result that there is a tendency for the platens to come closer together (preliminary results on materials reinforced with *inextensible* fibres were established by Saccomandi and Beatty [14]). This is shown in Sect. 4, where we also fit the data of Janmey et al. [7] to some of our models.

The novelty here then is the prediction of a negative Poynting effect of the same order of magnitude as the shear stress when soft tissue is sheared in the physiological range of strain (as in the experiments of Janmey et al. [7]), which is explained by a simple physical mechanism (Fig. 1). Although the predictions are only for three special modes of shear for three polynomial models, one can justify this claim by noting that the shearing deformations considered are essentially *canonical shearing modes*, in that every shearing deformation can be considered a non-linear superposition of these modes and the strain energies are likely to be representative of the mechanical response of soft tissue, as argued earlier.

2 Simple shear of soft tissues and material models

We call (X_1, X_2, X_3) and (x_1, x_2, x_3) the Cartesian coordinates of a typical particle in the undeformed and deformed configurations respectively. Then $\boldsymbol{F} \equiv \partial \boldsymbol{x} / \partial \boldsymbol{X}$ is the deformation gradient tensor (with $J \equiv \det(\boldsymbol{F})$), and $\boldsymbol{B} = \boldsymbol{F}\boldsymbol{F}^{\mathrm{T}}$ and $\boldsymbol{C} = \boldsymbol{F}^{\mathrm{T}}\boldsymbol{F}$ are the left and right Cauchy–Green deformation tensors respectively. The corresponding principal *isotropic invariants* are defined by
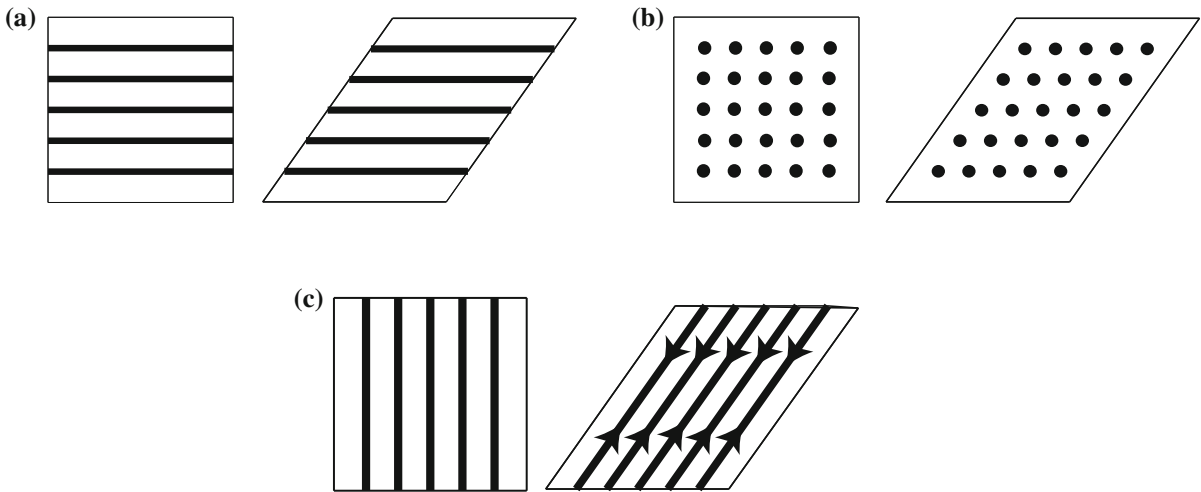
Fig. 1 Schematics of **a** longitudinal shear, **b** transverse shear and **c** perpendicular shear. In **a** and **c**, the *dark lines* represent the fibres. In **b**, the *darkened circles* denote fibres out of the plane of the page. The *arrows* in **c** indicate the resistive forces developing in the stretched fibres in response to the simple shear: this shear mode provides a simple mechanism to model negative Poynting effects

$$I_1 = \mathrm{tr}(\boldsymbol{B}), \quad I_2 = \tfrac{1}{2}\big[I_1^2 - \mathrm{tr}(\boldsymbol{B}^2)\big], \quad I_3 = \det(\boldsymbol{B}) = J^2. \tag{1}$$

Consider now a transversely isotropic, non-linearly elastic material with a preferred direction $\boldsymbol{M}$ in the undeformed configuration, physically induced by the presence of parallel fibres embedded in a softer elastic matrix. The so-called *anisotropic invariants* are defined as

$$I_4 = \boldsymbol{M} \cdot \boldsymbol{C}\boldsymbol{M}, \qquad I_5 = \boldsymbol{M} \cdot \boldsymbol{C}^2 \boldsymbol{M}. \tag{2}$$

As is well known, I_4 is the square of the stretch experienced by material elements in the fibre direction: when $I_4 \geq 1$, the fibres are stretched; when $I_4 \leq 1$, they are compressed.

As the material is assumed perfectly incompressible, $I_3 \equiv 1$, and the strain energy density W is therefore a function of only four invariants: $W = W(I_1, I_2, I_4, I_5)$. The corresponding constitutive law has the form [15]

$$\boldsymbol{\sigma} = -p\boldsymbol{I} + 2W_1\boldsymbol{B} - 2W_2\boldsymbol{B}^{-1} + 2W_4\boldsymbol{F}\boldsymbol{M} \otimes \boldsymbol{F}\boldsymbol{M} + 2W_5\left(\boldsymbol{F}\boldsymbol{M} \otimes \boldsymbol{B}\boldsymbol{F}\boldsymbol{M} + \boldsymbol{B}\boldsymbol{F}\boldsymbol{M} \otimes \boldsymbol{F}\boldsymbol{M}\right), \tag{3}$$

where $\boldsymbol{\sigma}$ denotes the Cauchy stress, attached subscripts denote partial differentiation of W with respect to the appropriate invariant and p is an arbitrary scalar field. To ensure that the stress is identically zero in the undeformed configuration, we require that

$$2W_1^0 - 2W_2^0 = p^0, \quad W_4^0 + 2W_5^0 = 0, \tag{4}$$

where the 0 superscript denotes evaluation in the reference configuration, in which $I_1 = I_2 = 3$, $I_4 = I_5 = 1$. It will also be assumed that the strain energy vanishes in the undeformed configuration, i.e. that $W^0 = 0$.

Merodio and Ogden [16] and Murphy [12] obtained restrictions to ensure the compatibility of the linear and non-linear theories. This compatibility requires that

$$2W_1^0 + 2W_2^0 = \mu_T, \quad 2W_5^0 = \mu_L - \mu_T, \quad 4W_{44}^0 + 16W_{45}^0 + 16W_{55}^0 = E_L + \mu_T - 4\mu_L, \tag{5}$$

where μ_T, μ_L are the infinitesimal shear moduli for shearing in planes normal to the fibres and along the fibres respectively, and E_L is the Young's modulus in the fibre direction (see Vergori et al. [17] for compatibility formulas in orthotropic and monoclinic elasticity).

There is significant experimental evidence, particularly for muscles (e.g. Gennisson [18], Papazoglou et al. [19], Sinkus et al. [20]), suggesting that

$$\mu_L > \mu_T, \tag{6}$$

with an order-of-magnitude difference recorded in some instances. There is a distinct lack of comprehensive experimental data for soft tissue where biaxial testing is combined with shear testing. One notable recent exception is the work of Morrow et al. [21], who showed that

$$E_L \gg \mu_L \tag{7}$$

for the *extensor digitorum longus* muscles of rabbits. These inequalities between the material constants are assumed to hold in what follows.

The signs of the partial derivatives of the strain-energy function will play an important role in the following analysis. For *isotropic* materials, the so-called empirical inequalities, given by

$$W_1 > 0, \quad W_2 \geq 0, \tag{8}$$

are often enforced. They are classically employed for rubber-like materials to ensure that specific choices for the strain-energy function give physically realistic mechanical responses (see Truesdell and Noll [22] and Beatty [23] for a discussion). In the absence of experimental data to suggest otherwise, they are assumed to hold also for our transversely isotropic materials.

Now note that strain energies which are additively decomposed into separate isotropic and anisotropic components, i.e. strain energies of the form

$$W = f(I_1, I_2) + g(I_4, I_5), \tag{9}$$

say, are consistent with linear theory, in the sense that no restrictions are imposed on the material constants μ_T, μ_L, E_L by assuming such a form. For simplicity in what follows, separable forms are assumed. Simple polynomial models can be adopted for transversely isotropic soft tissue, where the strain energies are at least quadratic in I_4 and I_5 and at least linear in I_1 and I_2. Murphy [12] and Feng et al. [24] have argued that it is essential that the strain-energy function be a function of both anisotropic invariants when modelling soft tissue, and we assume this here, in addition to assuming a dependence on the two isotropic invariants. These considerations lead to the following simple models of transversely isotropic response:

$$
\begin{aligned}
W^I &= \tfrac{1}{2}\mu_T\left[\alpha(I_1 - 3) + (1 - \alpha)(I_2 - 3)\right] \\
&\quad + \tfrac{1}{2}(\mu_T - \mu_L)(2I_4 - I_5 - 1) + \tfrac{1}{32}(E_L + \mu_T - 4\mu_L)(I_5 - 1)^2, \\
W^{II} &= \tfrac{1}{2}\mu_T\left[\alpha(I_1 - 3) + (1 - \alpha)(I_2 - 3)\right] \\
&\quad + \tfrac{1}{2}(\mu_T - \mu_L)(2I_4 - I_5 - 1) + \tfrac{1}{16}(E_L + \mu_T - 4\mu_L)(I_4 - 1)(I_5 - 1), \\
W^{III} &= \tfrac{1}{2}\mu_T\left[\alpha(I_1 - 3) + (1 - \alpha)(I_2 - 3)\right] \\
&\quad + \tfrac{1}{2}(\mu_T - \mu_L)(2I_4 - I_5 - 1) + \tfrac{1}{8}(E_L + \mu_T - 4\mu_L)(I_4 - 1)^2,
\end{aligned}
\tag{10}
$$

where $0 < \alpha \leq 1$ ([12] first introduced these models with $\alpha = 1$). The linear dependence on the first two strain invariants in (10) reflects the isotropic matrix response of a Mooney–Rivlin model.

The last of these models is a generalisation of the so-called standard reinforcing model:

$$W = c_1 (I_1 - 3) + c_2 (I_4 - 1)^2 \tag{11}$$

(where c_1 and c_2 are two positive material parameters), which is often used in the literature to illustrate fibre reinforcement. We thus call the last model of (10) the compatible standard reinforcing model. In addition to the standard reinforcing model (11), we make use of the (non-polynomial) Holzapfel–Gasser–Ogden model:

$$W = \frac{1}{2}\mu(I_1 - 3) + \frac{k_1}{2k_2} \left\{ \exp\left(k_2 (I_4 - 1)^2 \right) - 1 \right\}, \tag{12}$$

where μ, k_1, k_2 are positive material parameters (Holzapfel et al. [25]); this model is very popular for modelling biological soft tissues. These two models have a strain energy that depends only on I_1, I_4. We show in Sect. 4 that a dependence of W on I_2 is crucial to capturing the Poynting effect. In anticipation, we now introduce a modification of these models to include a Mooney–Rivlin response for the isotropic matrix:

$$W^{\mathrm{IV}} = c_1 \left[\alpha (I_1 - 3) + (1 - \alpha) (I_2 - 3) \right] + c_2 (I_4 - 1)^2, \tag{13}$$
$$W^{\mathrm{V}} = \frac{1}{2}\mu \left[\alpha (I_1 - 3) + (1 - \alpha) (I_2 - 3) \right] + \frac{k_1}{2k_2} \left\{ \exp\left(k_2 (I_4 - 1)^2 \right) - 1 \right\},$$

where $0 < \alpha < 1$. The first of these was introduced by Le Tallec [26] and was used by Horgan and Murphy [9] to demonstrate positive and negative Poynting effects in simple shear; the second one is used in the finite-element code ADINA [27].

3 Stress components in three shear modes

To investigate the non-linear shear response of passive ventricular myocardium, Dokos et al. [13] used cuboids of fibre-reinforced material with a family of parallel fibres aligned with two opposite parallel faces of a block. As sketched in Fig. 1, there are three distinct physical shear responses: (a) shearing in the direction of the fibres, which we call longitudinal shear; (b) shearing in the planes normal to the fibres, which we call transverse shear; and (c) shearing across the fibres, which we call perpendicular shear.

The invariants and Cauchy stress components for each of these deformations are given next using the Cartesian representations for the deformations given in [12], where it was assumed that the Z-axis was aligned in the direction of the fibres in the reference configuration. In each case the normal stress to the plane of shear is assumed to be identically zero.

3.1 Longitudinal shear

This shearing mode can be described by the deformation

$$x = X, \quad y = Y, \quad z = Z + \kappa X, \tag{14}$$

giving

$$I_1 = I_2 = 3 + \kappa^2, \quad I_4 = 1, \quad I_5 = 1 + \kappa^2. \tag{15}$$

Note that the fibres are not stretched in this shearing mode. The corresponding non-zero Cauchy stress components are then obtained from (3) as

$$
\sigma_{xx} = -p + 2W_1 - 2W_2\left(1 + \kappa^2\right),
$$
$$
\sigma_{yy} = -p + 2W_1 - 2W_2,
$$
$$
\sigma_{xz} = 2\kappa\left(W_1 + W_2 + W_5\right),
$$
$$
\sigma_{zz} = -p + 2W_1\left(1 + \kappa^2\right) - 2W_2 + 2W_4 + 4W_5\left(1 + \kappa^2\right).
$$
(16)

Assuming plane stress conditions, i.e. assuming that $\sigma_{yy} \equiv 0$, determines p as $p = 2W_1 - 2W_2$. The remaining normal stress components are therefore

$$
\sigma_{xx} = -2W_2\kappa^2, \qquad \sigma_{zz} = 2W_1\kappa^2 + 2W_4 + 4W_5\left(1 + \kappa^2\right).
$$
(17)

The normal stress component σ_{xx} is the force per current unit area which must be exerted on the x-planes in order to maintain the state of simple shear described in (14). Its sign is determined by the sign of W_2. The shear stress component σ_{xz} is the force per unit area which must be applied in the x-direction.

3.2 Transverse shear

This deformation can be described as follows:

$$
x = X + \kappa Y, \quad y = Y, \quad z = Z,
$$
(18)

so that

$$
I_1 = I_2 = 3 + \kappa^2, \quad I_4 = 1, \quad I_5 = 1.
$$
(19)

Again, there is no stretch occurring in the fibre direction. The Cauchy stress components are

$$
\sigma_{xx} = -p + 2W_1\left(1 + \kappa^2\right) - 2W_2,
$$
$$
\sigma_{xy} = 2\kappa\left(W_1 + W_2\right),
$$
$$
\sigma_{yy} = -p + 2W_1 - 2W_2\left(1 + \kappa^2\right),
$$
$$
\sigma_{zz} = -p + 2W_1 - 2W_2 + 2W_4 + 4W_5.
$$
(20)

Assuming plane stress conditions means that $\sigma_{zz} \equiv 0$ and, therefore, that

$$
\sigma_{xx} = 2W_1\kappa^2 - 2W_4 - 4W_5, \quad \sigma_{yy} = -2W_2\kappa^2 - 2W_4 - 4W_5.
$$
(21)

Here, the σ_{yy} term is the force per unit area which needs to be applied in the direction normal to the shearing platens in order to maintain simple shear, whereas σ_{xy} is applied in the direction of shear.

3.3 Perpendicular shear

This mode of shear can be described by deformations of the form

$$x = X + \kappa Z, \quad y = Y, \quad z = Z, \tag{22}$$

giving

$$I_1 = I_2 = 3 + \kappa^2, \quad I_4 = 1 + \kappa^2, \quad I_5 = \left(1 + \kappa^2\right)^2 + \kappa^2. \tag{23}$$

Note that perpendicular shear is the only mode of simple shear in which the fibres are stretched ($I_4 > 1$). Since the fibres are much stiffer than the matrix in which they are embedded, Fig. 1c suggests that a *tensile* normal force must be applied to the upper and lower surfaces of the specimen to simultaneously stretch the fibres and maintain the specimen in a state of simple shear. Tensile normal forces are equivalent to a negative Poynting effect, and perpendicular shear is proposed here as a simple explanation for the mechanism underlying the negative Poynting effect seen in the experiments of Janmey et al. [7]. This is discussed further in Sect. 4.

The non-zero Cauchy stress components for this deformation are

$$\sigma_{xx} = -p + 2W_1 \left(1 + \kappa^2\right) - 2W_2 + 2W_4\kappa^2 + 4W_5\kappa^2 \left(2 + \kappa^2\right),$$
$$\sigma_{yy} = -p + 2W_1 - 2W_2, \tag{24}$$
$$\sigma_{xz} = 2\kappa \left[W_1 + W_2 + W_4 + W_5 \left(3 + 2\kappa^2\right)\right],$$
$$\sigma_{zz} = -p + 2W_1 - 2W_2 \left(1 + \kappa^2\right) + 2W_4 + 4W_5 \left(1 + \kappa^2\right).$$

Setting $\sigma_{yy} \equiv 0$ yields p, and therefore

$$\sigma_{xx} = 2\kappa^2 \left[W_1 + W_4 + 2W_5 \left(2 + \kappa^2\right)\right], \quad \sigma_{zz} = -2W_2\kappa^2 + 2W_4 + 4W_5 \left(1 + \kappa^2\right). \tag{25}$$

In this case it is the σ_{zz} term that determines the force which needs to be applied in the direction normal to the shearing platens in order to maintain simple shear, whereas σ_{xz} is applied in the direction of shear.

4 The Poynting effect

The normal forces needed to maintain simple shear for each of the three shearing modes derived in the previous section are of interest here. Call the necessary normal stresses for longitudinal, transverse and perpendicular shear $\mathcal{N}_L$, $\mathcal{N}_T$ and $\mathcal{N}_P$ respectively. Collecting the results of the last section together, these are thus given by

$$\mathcal{N}_L = -2W_2\kappa^2,$$
$$\mathcal{N}_T = -2W_2\kappa^2 - 2W_4 - 4W_5, \tag{26}$$
$$\mathcal{N}_P = -2W_2\kappa^2 + 2W_4 + 4W_5 \left(1 + \kappa^2\right).$$

Many models of transversely isotropic soft tissue assume strain-energy functions which are independent of I_2 for simplicity. However, as we can see from (26), these models implicitly assume a Poynting effect which is identically zero in longitudinal shear, a prediction which seems unduly prescriptive and for which there is no experimental justification. Hence, in particular, the standard reinforcing model (11) and the Holzapfel–Gasser–Ogden model (12)

cannot account for a Poynting effect in longitudinal shear. If, as is almost certainly the case in practice, $W_2 > 0$, then a compressive force must be applied, or otherwise the material would expand normal to the direction of shear. This corresponds to the usual *positive Poynting effect*. For *isotropic* materials, the crucial role of this dependence on the second invariant was pointed out explicitly by Horgan and Murphy [9], Horgan and Smayda [6] and Mihai and Goriely [4].

Next we note that for separable strain-energy functions (9) in transverse shear (for which $I_4 = I_5 = 1$) we have

$$2W_4 + 4W_5 = 2g_4(1, 1) + 4g_5(1, 1) = 0, \tag{27}$$

because of the initial condition (4)$_2$. On using this condition in the second of (26), we see that there are just two modes of normal stress response, the effectively isotropic response

$$\mathcal{N}_{\text{iso}} = \mathcal{N}_{\text{L}} = \mathcal{N}_{\text{T}} = -2W_2\kappa^2, \tag{28}$$

and the perpendicular shear anisotropic response $\mathcal{N}_{\text{P}}$.

By virtue of the empirical inequalities (8), $\mathcal{N}_{\text{iso}} \leq 0$, so that we have the usual positive Poynting effect for materials with additively split strain energies in longitudinal and transverse shear, if the strict inequality sign holds. Since the anisotropic invariants are associated with the stiff reinforcing fibres, as reflected in the linearisation condition (5)$_3$ for example, it also seems reasonable to assume that

$$W_4 \ \text{ or } \ W_5 \gg W_1, W_2. \tag{29}$$

If these constitutive inequalities hold, then it follows that $\mathcal{N}_{\text{P}} > 0$, so that we have a possible *negative Poynting effect in perpendicular shear*.

Thus, both positive and negative Poynting effects are likely for soft tissue reinforced with macromolecular fibrils, and the magnitude of the negative effect is expected to be much larger. These predictions are supported by consideration of specific strain energies, as shown next.

First note that the isotropic response is the same for all three materials of the polynomial form $W^{\text{I}} - W^{\text{III}}$ in (10) and is given by

$$\mathcal{N}_{\text{iso}} = \mu_{\text{T}} (\alpha - 1) \kappa^2 < 0. \tag{30}$$

Thus, a compressive force must be applied to the top and bottom surfaces of the sheared specimen to counteract the tendency of these materials to expand in the direction normal to the direction of the applied shear force. Hence, the classical (positive) Poynting effect occurs for both transverse and longitudinal shears.

Using an obvious notation, the anisotropic normal response in perpendicular shear of the three models is given by

$$\mathcal{N}_{\text{P}}^{\text{I}} = \left[\mu_{\text{T}} (\alpha - 3) + 2\mu_{\text{L}} + \tfrac{1}{4}(E_{\text{L}} + \mu_{\text{T}} - 4\mu_{\text{L}}) \left(1 + \kappa^2 \right) \left(3 + \kappa^2 \right) \right] \kappa^2,$$

$$\mathcal{N}_{\text{P}}^{\text{II}} = \left[\mu_{\text{T}} (\alpha - 3) + 2\mu_{\text{L}} + \tfrac{1}{8}(E_{\text{L}} + \mu_{\text{T}} - 4\mu_{\text{L}}) \left(5 + 3\kappa^2 \right) \right] \kappa^2, \tag{31}$$

$$\mathcal{N}_{\text{P}}^{\text{III}} = \left[\mu_{\text{T}} \left(\alpha - \tfrac{5}{2} \right) + \tfrac{1}{2} E_{\text{L}} \right] \kappa^2.$$

Now let $\mathcal{N}/\mu_{\text{T}}$ be a dimensionless measure of the normal stress. For a physiological range of strain, each of the normalised normal stresses for perpendicular shear is plotted in Fig. 2 for

Fig. 2 Normal stress
responses accompanying
perpendicular shear (*dashed
lines*) and the isotropic
transverse and longitudinal
shear (*full line*) for three
models of solids reinforced
with one family of fibres
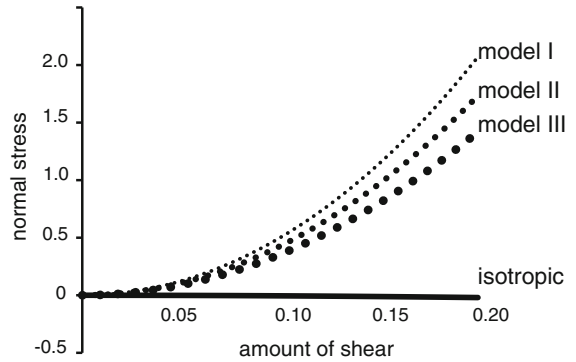
- $\alpha = 1/2$, corresponding to the middle of the range of the parameter;
- $\mu_L/\mu_T = 5$, corresponding to a typical relationship between the shear moduli for the experimental data given in Gennisson [18], Papazoglou et al. [19], Sinkus et al. [20];
- $E_L/\mu_T = 75$, motivated by the data of Morrow et al. [21].

The normalised isotropic response (30) is also plotted in Fig. 2 for $\alpha = 1/2$.

Recall that a positive (tensile) normal stress corresponds to the *negative* or reverse Poynting effect. From Fig. 2 we see that perpendicular shear is accompanied by a *negative* Poynting effect and that, relative to the perpendicular shear response, the Poynting effect accompanying transverse and longitudinal shear is approximately zero [although in absolute terms, there is a (small) positive Poynting effect]. Therefore, the magnitude of the negative Poynting effect dominates the positive effect when soft tissue is sheared. From Fig. 2 it is also seen that the tensile normal stress is monotonically increasing with respect to the amount of shear.

The relative magnitudes of the normal stresses with respect to the applied shear stresses are now investigated. Define the dimensionless quantity

$$\mathcal{R} \equiv \frac{\sigma_{\text{normal}}}{\sigma_{\text{shear}}}. \tag{32}$$

For simplicity, we only consider the so-called sompatible standard reinforcing model (Model III, given by $(10)_3$) since it gives rise to the smallest normal stress response for perpendicular shear (see Fig. 2 above). The corresponding longitudinal, transverse and perpendicular shear stresses are

$$\sigma_{\text{shear}}^L = \mu_L \kappa, \qquad \sigma_{\text{shear}}^T = \mu_T \kappa, \qquad \sigma_{\text{shear}}^P = \mu_L \kappa + \tfrac{1}{2}(E_L - 3\mu_T)\kappa^3, \tag{33}$$

respectively. The corresponding $\mathcal{R}$ for each mode of shear is therefore

$$\mathcal{R}^L = \frac{\mu_T}{\mu_L}(\alpha - 1)\kappa, \quad \mathcal{R}^T = (\alpha - 1)\kappa, \quad \mathcal{R}^P = \frac{[\mu_T(2\alpha - 5) + E_L]\kappa}{2\mu_L + (E_L - 3\mu_T)\kappa^2}, \tag{34}$$

respectively. For the material parameters used previously, these ratios are plotted in Fig. 3.

Thus, even for the restricted amount of shear considered (in line with physiological strains of the order of 10 %), a physically significant reverse Poynting effect is shown to accompany perpendicular shearing deformations, with the corresponding effect for the other two modes of shear relatively unimportant. Indeed for the upper range of shear considered, it is seen that the tensile normal stress in perpendicular shear is of the same order of magnitude as the shearing stress. Although the existence of a substantial Poynting effect in soft tissue awaits experimental confirmation, the data of Janmey et al. [7] for semi-flexible biopolymer gels confirm the existence of a Poynting effect of this order of magnitude. This suggests that the Poynting effect could be an important physiological control mechanism, for example.
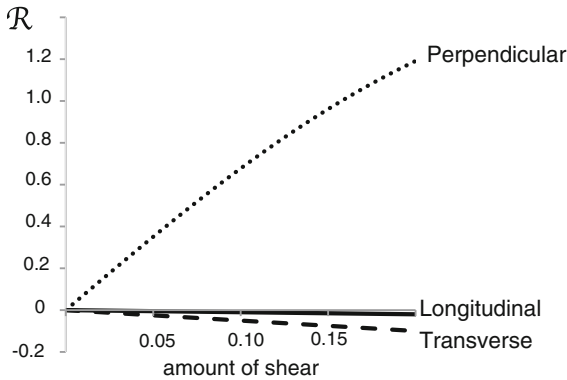
Fig. 3 Plots of $\mathcal{R}$ (relative magnitude of normal stress with respect to applied shear stress) for different shearing modes of one model of a solid reinforced with one family of fibres
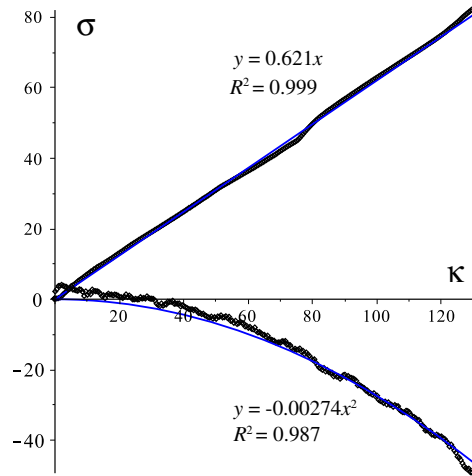
Fig. 4 Data of Janmey et al. [7] for shearing of a block of gel made from actin cross-linked by polyacrylamide, displaying a linear shear stress amount of shear relationship and a quadratic normal stress amount of shear relationship. More than 260 measurements were recorded. The negative sign of the normal stress indicates the classical (positive) Poynting effect. The actual values are unimportant, as both the stress and strain are computed up to multiplicative constants (see for instance the ARES rheometer manual[28])

Finally, we analyse two of the data sets presented by Janmey et al. [7]: one exhibiting the positive Poynting effect, the other the reverse Poynting effect. When shearing a block of gel made from actin cross-linked by polyacrylamide, Janmey et al. [7] observed a positive Poynting effect. In Fig. 4 we see that the fitting of the shear and normal stress components to linear and quadratic trends respectively gives excellent results ($R^2 = 0.999, 0.987$ respectively), i.e. that the material constitutive law obeys

$$\sigma_{\text{shear}} = a\kappa, \qquad \sigma_{\text{normal}} = -b\kappa^2, \tag{35}$$

for some positive constants a and b. If the polyacrylamide gel is an isotropic material, then (35) clearly indicates that it could be modelled as a Mooney–Rivlin material. If it is a transversely isotropic material, and biaxial testing is the most efficient way of determining this, then the data reported in the figure cannot correspond to perpendicular shear (which would not give a positive Poynting effect). However, polyacrylamide could be modelled with the strain energies W^{I}–W^{V} of (10) and (13) as subjected to transverse shear because all models predict σ_{shear} and σ_{normal} of the form (35). It could also have been subjected to longitudinal shear because all models predict σ_{shear} and σ_{normal} of the form (35), except for model W^{I}, which gives $\sigma_{\text{shear}}^{\text{I}}$ as an odd cubic in κ.

In Fig. 5 we present the data collected by Janmey et al. [7], showing a reverse Poynting effect for the shear of a block of gel crossed-linked with collagen. This phenomenon cannot be captured by isotropic models (unless the empirical inequalities (8) are violated). For transverse isotropy, we have perpendicular shear at our disposal to model the data. We used in turn the five models W^{I}–W^{V} of (10) and (13) and found that W^{I} provided the best fit ($R^2 = 0.978$) (see figure). We used (31)$_1$ as an objective function, writing $\mathcal{N}_{\text{P}}^{\text{I}}$ as $\mathcal{N}_{\text{P}}^{\text{I}} = a\kappa^2 + b(4\kappa^4 + \kappa^6)$, where a and b are best-fit parameters to be determined. Of course, we acknowledge that the fitting exercise has its limitations, given that the data are not smooth and we have no way of knowing whether this particular gel was both transversely isotropic and subjected to perpendicular shear.

Fig. 5 Normal stress vs. amount of shear from data of Janmey et al. [7] for shearing of a block of gel made from actin cross-linked by collagen. Approximately 50 measurements were recorded. The (mostly) positive sign of the normal stress indicates a reverse (negative) Poynting effect. The actual values are unimportant because both the stress and the strain are computed up to multiplicative constants (see for instance [28]). The experimental data are fitted with model (31)$_1$ in perpendicular shear

$$y = 0.0393x^2 + 6.24 \times 10^{-8}(4x^4 + x^6)$$

$$R^2 = 0.978$$
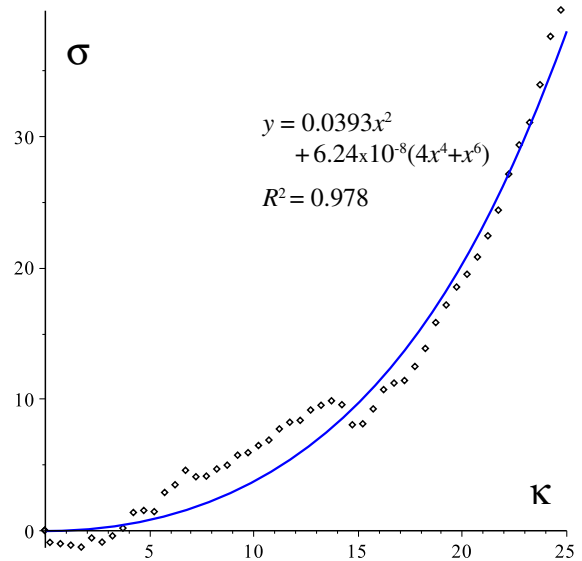
5 Conclusion

The simple analysis presented here, which assumes that plane stress conditions hold when shearing, suggests that for soft tissue a negative (reverse) Poynting effect should occur for perpendicular shear, with the positive effect accompanying the other two modes being relatively unimportant. It has been demonstrated that the negative Poynting effect could be quite substantial, of the same order of magnitude of the applied shearing stress for physiological strains, in some circumstances. Although these results are consistent with experimental data of Janmey et al. [7] for hydrogels, further experimental work on biotissues is clearly desirable.

References

1. British Standard BS ISO 8013:2006 Rubber, vulcanized—determination of creep in compression or shear
2. Poynting JH (1909) On pressure perpendicular to the shear planes in finite pure shears, and on the lengthening of loaded wires when twisted. Proc R Soc Lond Ser A 82:546–559
3. Rivlin RS (1948) Large elastic deformation of isotropic materials iv: further developments of the general theory. Philos Trans R Soc Lond Ser A 241:379–397
4. Mihai LA, Goriely A (2011) Positive or negative poynting effect? the role of adscititious inequalities in hyperelastic materials. Proc R Soc Lond A 467:3633–3646
5. Destrade M, Murphy JG, Saccomandi G (2012) Simple shear is not so simple. Int J Non-Linear Mech 47:210–214
6. Horgan CO, Smayda M (2012) The importance of the second strain invariant in the constitutive modeling of elastomers and soft biomaterials. Mech Mater 51:43–52
7. Janmey PA, McCormick ME, Rammensee S, Leight JL, Georges PC, MacKintosh FC (2007) Negative normal stress in semiflexible biopolymer gels. Nat Mater 6:48–51
8. Destrade M, Gilchrist MD, Motherway J, Murphy JG (2012) Slight compressibility and sensitivity to changes in Poisson's ratio. Int J Numer Methods Eng 90:403–411
9. Horgan CO, Murphy JG (2011) On the normal stresses in simple shearing of fiber-reinforced nonlinearly elastic materials. J Elast 104:343–355
10. Wu MS, Kirchner HOK (2010) Nonlinear elasticity modeling of biogels. J Mech Phys Solids 58:300–310
11. Spencer AJM (1984) Constitutive theory for strongly anisotropic solids. In Spencer AJM (ed) Continuum theory of the mechanics of fibre-reinforced composites. CISM Courses and Lectures Series No. 282. Springer-Verlag, Vienna

12. Murphy JG (2013) Transversely isotropic biological, soft tissue must be modelled using both anisotropic invariants. Eur J Mech A/Solids 42:90–96
13. Dokos S, Smaill BH, Young AA, LeGrice IJ (2002) Shear properties of passive ventricular myocardium. Am J Physiol Heart Circ Physiol 283:H2650–H2659
14. Saccomandi G, Beatty MF (2002) Universal relations for fiber-reinforced elastic materials. Math Mech Solids 7:95–110
15. Ogden RW (2003) Nonlinear elasticity, anisotropy, material stability and residual stresses in soft tissue. In Biomechanics of soft tissue in cardiovascular systems. CISM Courses and Lectures Series No. 441. Springer, Vienna, pp 65–108
16. Merodio J, Ogden RW (2005) Mechanical response of fiber-reinforced incompressible non-linearly elastic solids. Int J Non-Linear Mech 40:213–227
17. Vergori L, Destrade M, McGarry P, Ogden RW (2013) On anisotropic elasticity and questions concerning its finite element implementation. Comput Mech 52:1185–1197
18. Gennisson J-L, Catheline S, Chaffaõ S, Fink M (2003) Transient elastography in anisotropic medium: application to the measurement of slow and fast shear wave speeds in muscles. J Acoust Soc Am 114:536–541
19. Papazoglou S, Rump J, Braun J, Sack I (2006) Shear wave group velocity inversion in MR elastography of human skeletal muscle. Magn Reson Med 56:489–497
20. Sinkus R, Tanter M, Catheline S, Lorenzen J, Kuhl C, Sondermann E, Fink M (2005) Imaging anisotropic and viscous properties of breast tissue by magnetic resonance-elastography. Magn Reson Med 53:372–387
21. Morrow DA, Haut Donahue TL, Odegard GM, Kaufman KR (2010) Transversely isotropic tensile material properties of skeletal muscle tissue. J Mech Behav Biomed Mater 3:124–129
22. Truesdell C, Noll W (1965) The non-linear field theories of mechanics. In: Flugge S (ed) Encyclopedia of Physics, vol III/3, 3rd edn. Springer-Verlag, Berlin
23. Beatty MF (1989) Topics in finite elasticity: hyperelasticity of rubber, elastomers, and biological tissue. Appl Mech Rev 40:1699–1734
24. Feng Y, Okamoto RJ, Namani R, Genin GM, Bayly PV (2013) Measurements of mechanical anisotropy in brain tissue and implications for transversely isotropic material models of white matter. J Mech Behav Biomed Mater 23:117–132
25. Holzapfel GA, Gasser TC, Ogden RW (2000) A new constitutive framework for arterial wall mechanics and a comparative study of material models. J Elast 61:1–48
26. Le Tallec P (1994) Numerical methods for nonlinear three-dimensional elasticity. In: Ciarlet PG, Lions JL (eds) Handbook of Numerical Analysis, vol III. Elsevier, Amsterdam
27. ADINA R&D Inc (2005) ADINA theory and modeling guide. ADINA R&D Inc, Watertown
28. ARES Rheometer manual (2006) Rheometrics series user manual. Revision J, TA Instrument-Waters LLC, New Castle